Chinese Chemical Letters 34 (2023) 107207

Contents lists available at ScienceDirect

Chinese Chemical Letters

journal homepage: www.elsevier.com/locate/cclet

$[Cd(Sn_9)_2]^{6-}$ and $[Cd(Ni@Sn_9)_2]^{6-}$: Reactivity and coordination chemistry of empty and Ni-centered $[Sn_9]^{4-}$ Zintl ions

Ya-Nan Yang, Lei Qiao*, Zhong-Ming Sun*

State Key Laboratory of Elemento-Organic Chemistry, Tianjin Key Lab of Rare Earth Materials and Applications, School of Material Science and Engineering, Nankai University, Tianjin 300350, China

ARTICLE INFO

Article history:
Received 10 January 2022
Revised 4 February 2022
Accepted 8 February 2022
Available online 11 February 2022

Keywords:
Heterometallic complexes
Sn cluster
Zintl anions
DFT calculation
Electronic structure

ABSTRACT

To investigate the reactivity of homoatomic clusters $[E_9]^{4-}$ (E = Si-Pb) and intermetalloid clusters $[M@E_9]^{q-}$, the reactions of the Zintl anions $[Sn_9]^{4-}$ and $[Ni@Sn_9]^{4-}$ with the $CdMes_2$ (Mes = Mesitylene) in the presence of 2.2.2-crypt were carried out. Two new compounds $[K(2.2.2\text{-crypt})]_6[(Sn_9)Cd(Sn_9)]\cdot en$ (**1**) and $[K(2.2.2\text{-crypt})]_6[(Ni@Sn_9)Cd(Ni@Sn_9)]\cdot en$ (**2**) were afforded. Both **1** and **2** were characterized by single-crystal X-ray diffraction, energy dispersive X-ray (EDX), and electrospray ionization mass spectrometry (ESI-MS), and can be viewed as two $[Sn_9]^{4-}$ or $[Ni@Sn_9]^{4-}$ subunits bridged by Cd ion in an η^3:η^3 coordination mode. Quantum chemical calculations reveal the relationships between the geometries and electronic structures of clusters **2a**, $[Ni_3Ge_{18}]^{4-}$ and $[Cu_4@Sn_{18}]^{4-}$. Further electron localization technique (AdNDP method) was performed to explain chemical bonding patterns of **1a**.

Group 14 Zintl ions have been investigated extensively in solution chemistry and nanomaterials during the last 20 years [1–5]. Homoatomic deltahedral clusters of $E_9{}^{4-}$ (E = Ge, Sn, Pb) are considered to be important precursors to react with the transition-metal reagents in an aprotic solvent, and previous studies have been mainly focused on the reactions of empty nine-atom cages with low-valent transition-metal compounds. One of the efficient strategies is that $[E_9]^{4-}$ anions are used as six-electron donors to replace the ligand of organometallic complexes leading to the formation of ten-vertex *closo*–clusters, in which the square plane of $[E_9]^{4-}$ is capped by organometallic fragments, for instance, $[Sn_9M(CO)_3]^{4-}$ (M = Cr, Mo, W) [6], $[Ge_9Ni(CO)]^{3-}$ [7], $[Ge_9Pd(PPh_3)]^{3-}$ [8], $[Sn_9Ir(COD)]^{3-}$ [9], $[Ge_9Cu(PR_3)]^{3-}$ ($R = {}^iPr$, Cy) [10] and $[E_9ZnR]^{3-}$ (R = Mes, ${}^iPr$, Ph) [11]. Moreover, as analogs of fullerene, nonatetrelide is capable of accommodating one transition metal atom by methods of solution reaction or high-temperature solid-state synthesis [12–16]. Nevertheless, due to the unique reactivity of endohedral clusters, only several $[M@E_9]^{q-}$ can be further reacted with suitable organometallic compounds to form "Rudolph's complexes", namely $[M@E_9ML]^{n-}$ (M = transition metal, L = ligand) [15,17,18].

A series of polymers, $[Ge_9\text{-}Ge_9]^{6-}$ [19], $[Ge_9{=}Ge_9{=}Ge_9]^{6-}$ [20] and nanorod $[Ge_9{=}Ge_9{=}Ge_9{=}Ge_9]^{8-}$ [21], were obtained by oxidative coupling reactions of monomer $Ge_9{}^{4-}$. And a family of clusters containing $Ge_9{}^{4-}$ and bridged metal atom has also been isolated, such as $[Ge_9InGe_9]^{5-}$ [22], one-dimension chain ${}^{1}_{\infty}[MGe_9]^{2-}$ (M = Zn, Hg) [23,24]. As for tin clusters, only three related examples, $[Sn_9HgSn_9]^{6-}$ [25], $[Sn_9AgSn_9]^{7-}$ [26] and $[Ag(Sn_9\text{-}Sn_9)]^{5-}$ [27] were discovered. Recently our group reported the first example of an endohedral bridged Zintl cluster $[(Ni@Sn_9)In(Ni@Sn_9)]^{5-}$ [28], which contains a bridged main group metal atom. Given the less explored chemistry of $[M@Sn_9]^{q-}$ and their similarity with the empty counterpart when they react with transition metals, based on the previous work, further research was carried out. Here, we present the synthesis and characterization of two new Zintl clusters $[(Sn_9)Cd(Sn_9)]^{6-}$ (**1a**) and $[(Ni@Sn_9)Cd(Ni@Sn_9)]^{6-}$ (**2a**) (Fig. 1), which proves that both empty and centered nine-atom tin clusters behave similarly to $CdMes_2$.

To investigate the different reactivities of the $[Sn_9]^{4-}$ and $[Ni@Sn_9]^{4-}$, we have tried to adjust the reaction conditions to isolate the corresponding complex. Since the synthesis process of **1** and **2** are in the same way, only the synthesis of **1** is taken as an example for description. When the required amount of $CdMes_2$ was added directly to a homogeneous solution of K_4Sn_9 with the chelating agent 2.2.2-crypt, the color of the solution rapidly changed from reddish-brown to dark red. After stirring for 3 h, the solution turned reddish-brown again. Carefully layered with toluene, crystals of compound **1** were obtained after two weeks. The electrospray ionization (ESI) mass spectra of the crystal sample

---

* Corresponding authors.
E-mail addresses: 1120180362@mail.nankai.edu.cn (L. Qiao), sunlab@nankai.edu.cn (Z.-M. Sun).

https://doi.org/10.1016/j.cclet.2022.02.013
1001-8417/

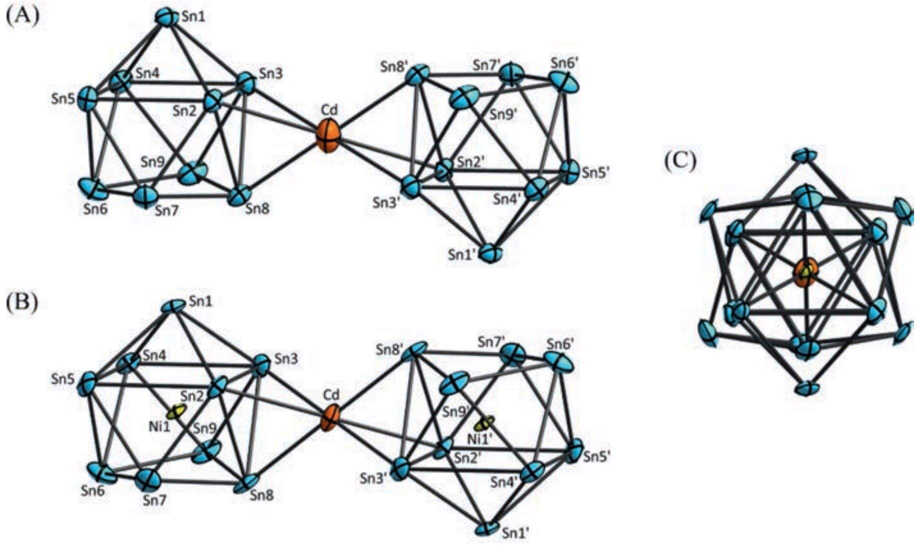

Fig. 1. Structure of clusters (A) **1a** and (B) **2a**. (C) Side view of **2a**. Atoms are shown with thermal ellipsoids set at 70% probability level.

of compound **2** shows the signals of $[KNiSn_9]^-$ ($m/z = 1166.0240$), $[NiSn_9]^-$ and $[NiSn_{10}]^-$ without the corresponding peaks of parent anion, similarly only the signal of $[Sn_9]^-$ is detected in the mass spectra of compound **1**. Such phenomenon, which was also observed in $[Ge_9SnGe_9]^{4-}$ [29], suggests that the Cd-Sn bonds are relatively weak in contrast to the previously reported In-Sn bond [28]. From the perspective of experimental results, the reactivity of $[Sn_9]^{4-}$ and $[Ni@Sn_9]^{4-}$ with $CdMes_2$ did not differ too much. Hence, given the above studies and the former conclusions, the formation of **1** and **2** is likely to undergo in solution first a simple ligand exchange reaction in which $Sn_9{}^{4-}$ replaces one Mes ligand of $CdMes_2$ to form $[Sn_9CdMes]$ units by a further replacement of $Sn_9{}^{4-}$ unit and finally compound **1** was formed [15,26,28,29,32].

Although compound **1** was plagued by continuous positional disorder at the $[(Sn_9)Cd(Sn_9)]^{6-}$ anion sites, the combination between X-ray single-crystal result of compound **2** and energy dispersive X-ray Spectroscopic (EDX) analyses confirm the presence of (Ni), Cd, and Sn and the ratio of them. In anions $[(Sn_9)Cd(Sn_9)]^{6-}$ and $[(Ni@Sn_9)Cd(Ni@Sn_9)]^{6-}$, the Cd atom is coordinated by two $[Sn_9]$ and $[Ni@Sn_9]$ subunits in an $\eta^3{:}\eta^3$ coordination mode forming sandwich complexes, and both have perfect inversion center at the cadmium atom position, which is analogous to $[Ge_9ZnGe_9]^{6-}$ and $[Sn_9HgSn_9]^{6-}$ [25,29].

Two $[Sn_9]^{4-}$ or $[Ni@Sn_9]^{4-}$ subunits adopt a mono-capped square antiprism structure. The Sn-Sn distances of **1a** are in the range of 2.9056(14) Å and 3.2826(15) Å, which are slightly shorter than those in $[Sn_9]^{4-}$ (2.928(6)-3.308(5) Å). For cluster **2a**, the Sn-Sn contacts and the Ni-Sn bond distances are normally compared to the reported $[Ni@Sn_9]^{4-}$ [13].

All of the Cd-Sn distances (2.8913–3.3246 Å in **1a** and 2.9658–3.2060 Å in **2a**) are significantly longer than the sum of single-bond covalent radii 2.76 Å and the Cd-Sn single bonds in $[MsSi\{SiMeN(p\text{-}Tol)\}_3Sn]_2Cd$ (2.676 Å) [30] and $[Cd(SnB_{11}H_{11})_4]^{6-}$ (av. 2.756 Å) [31], which indicates relatively weak Cd-Sn interactions. Interestingly, the distances of Cd-Sn8 in anion **1a** are shorter than those in **2a**, in contrast, the bond lengths of Cd-Sn2 and Cd-Sn3 are longer than those in **2a**. This trend of bond length averaging in **2a** may be due to the insertion of the Ni atoms. We also compared the bond lengths of **2a** with those in $[(Ni@Sn_9)In(Ni@Sn_9)]^{5-}$ and found that all of the Sn-Sn and Ni-Sn bonds in **2** are longer than those in $[K(2.2.2\text{-crypt})]_5[(Ni@Sn_9)In(Ni@Sn_9)]\cdot DMF$ (Full details of bond lengths are given in Table 1).

Table 1
Bond lengths (Å) comparison of **2a** and $[Ni@Sn_9]In[Ni@Sn_9]^{5-}$. ($Sn^a$: Sn4–6; Sn^b: Sn1, 7, 9; Sn^c: Sn2, 3, 8).

	$[(Ni@Sn_9)Cd(Ni@Sn_9)]^{6-}$	$[(Ni@Sn_9)In(Ni@Sn_9)]^{5-}$
Sn^a-Sn^a	3.0046–3.1740	2.9936–3.0551
Sn^a-Sn^b	3.0108–3.0695	2.9960–3.0542
Sn^b-Sn^c	2.9598–2.9968	2.9225–2.959
Sn^c-Sn^c	3.2222–3.323	3.2194–3.350
Ni-Sn	2.5678–2.7204	2.521–2.707
Cd-Sn	2.9658–3.2060	–
In-Sn	–	3.0508–3.1252

It is worth noting that cluster **2a** is similar to the known $[(Ni@Ge_9)Ni(Ni@Ge_9)]^{4-}$ [33] reported by Sevov from the view of the coordination way. Specifically, the central Cd and Ni ions of these two clusters coordinate respectively with two triangle faces of $Ni@E_9$ units ($E = Sn$ and Ge) to form an approximately octahedral environment. To understand the relationship between the geometries and electronic structures of these above-mentioned clusters, we performed density functional theory at the PBE0/def2tzvp level of theory [34,35]. The PCM polarizable conductor calculation model was performed with the solvent data for ethylenediamine ($\xi = 12.9$) to simulate the confining effects of the cationic environment in the solid-state in all cases [36,37]. Default convergence criteria were used for the optimization tasks with Gaussian 09 program. The initial structures for optimizations of cluster **2a** and $[(Ni@Ge_9)Ni(Ni@Ge_9)]^{4-}$ were taken from the experimentally observed structures (single-crystal X-ray diffraction analysis) with a restriction of D_{3d} symmetry by adjusting the coordinates, but their optimized results show C_{2h} and C_i symmetries, respectively. Full details of the Cartesian coordinates and the optimized bond lengths are given in Supporting information. The deviation between optimized bond lengths and those corresponding experimental values are within a reasonable 2% range, which is a common observation in calculations on zintl chemistry that may be due to the absence of an explicit crystal environment in the computational model. Frequency calculations confirmed that these optimized structures correspond to their respective minima in the potential energy surfaces. A comparison of the optimized geometries exhibits the superficial similarities between these related clusters, but also some subtle differences (Fig. 2). The most obvious difference is that the Cd-Ni contacts of 4.31 Å effectively confirm non-bonding interactions while the Ni-Ni distances of 2.43 Å

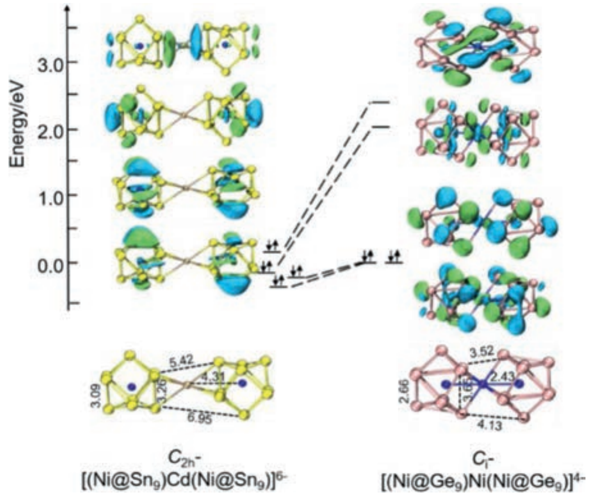

Fig. 2. Optimized structures of $[(Ni@Sn_9)Cd(Ni@Sn_9)]^{6-}$, $[(Ni@Ge_9)Ni(Ni@Ge_9)]^{4-}$ and the frontier Kohn–Sham orbitals of the two clusters. Iso-surface value = 0.03 a.u.

compare well with bonding distances in the corresponding clusters containing Ni-Ni bonds [38,39]. The more subtle differences appear in the shape of triangles that coordinated with the Cd/Ni atoms and the E-E distances between the two Ni@E$_9$ units. In cluster **2a**, the two Sn-Sn distances are 3.26 Å and 5.42 Å respectively, and the ratio between the two is 0.60. In contrast, the ratio of the two corresponding Ge-Ge distances is 1.04. In the D_{2h}-symmetric $[Cu_4@Sn_{18}]^{4-}$ optimized at the same level of theory, representing the two E$_9$ cages are complete fusion, the corresponding ratio is 1.55 (Fig. S16 in Supporting information) [40]. Hence, cluster **2a**, representing the completely separated state, can be viewed as a starting stage of fusion, which is further to form partly fusion cluster, such as $[(Ni@Ge_9)Ni(Ni@Ge_9)]^{4-}$, and finally to achieve the total coalescence defined by $[Cu_4@Sn_{18}]^{4-}$.

As for their electronic structures, the total cluster valence electrons of cluster **2a** and $[(Ni@Ge_9)Ni(Ni@Ge_9)]^{4-}$ are 110 and 106, respectively, indicating that two orbitals are occupied in the former but unoccupied in the latter. Hence, finding the two orbitals is very meaningful to understand those differences in structural chemistry. The HOMO of cluster **2a** is an anti-bonding orbital constituted by the HOMOs of two Ni@Sn$_9$ units, which is an in-phase combination of Sn 5p orbitals in each triangular face coordinated to the bridging Cd atom. In a related matter, the LUMO+1 of the Ni$_3$ cluster is mainly localized on the Ge$_9$ fragments. Although the LUMO+1 orbital is an out-of-phase combination between each coordination triangular face, the net bond order is only 1/6, indicating some interactions between the two Ge$_9$ units and between the three atoms of the coordination triangular faces. Hence, if two electrons are removed, the triangular face would be expanded, which is an above-mentioned difference in these clusters. For the HOMO-1, HOMO-2, and HOMO-3 of cluster **2a**, they do not show any interactions between the endohedrally encapsulated Ni ions and the bridging Cd atom, but a strong anti-bonding interaction in LUMO of Ni$_3$ cluster was presented (the in-phase combination of Ni 3d orbitals with the lower energy which means they are also occupied). Hence, these orbitals on the Ni-Ni bonding are consistent with those experimental observations. This is another structural difference mentioned above between the two clusters.

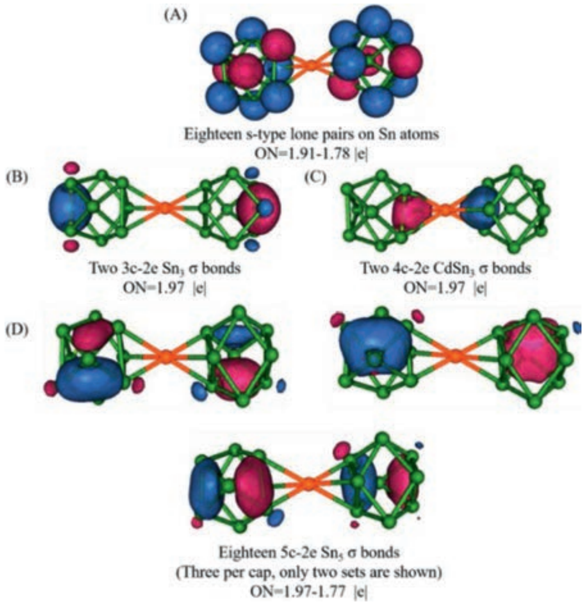

Fig. 3. Representative chemical bonding pictures and occupation numbers were obtained for cluster **1a**. ON denotes occupation number and is equal to 2.00 |e| in the ideal case of a doubly occupied bond. (A) Eighteen s-type lone pairs on Sn atoms; (B) Two 3c-2e Sn$_3$ σ bonds; (C) Two 4c-2e CdSn$_3$ σ bonds; (D) Eighteen 5c-2e Sn$_5$ σ bonds.

To further understand the chemical bonding pattern of the title clusters, the adaptive natural density partitioning algorithm (AdNDP) was performed by using Multiwfn 3.8 program [41,42]. Clusters **1a** and **2a** have a similar bonding situation because two embedded Ni ions can be considered as a zero-electron-donor to cluster bonding. Hence, we only analyze the bonding pictures of cluster **1a** for an example. Cluster **1a** has 90 valence electrons in total (18 × 4 |e| from 18 Sn atoms, 12 |e| from Cd atom and 6 |e| from the 6- cluster charge), providing 45 two-electron AdNDP bonding elements. The algorithm starts to search one-center two-electron elements, giving five D-type lone pairs (LPs) on Cd atom (Fig. S17 in Supporting information) and 18 s-type LPS on each Sn atom (Fig. 3A) with the occupied number (ON) of 1.99–2.00 |e| and 1.99–2.00 |e| respectively. Further search results found two 3c-2e σ bonds in Sn$_3$ triangular faces with ON = 1.97 |e| (Fig. 3B) and two 4c-2e σ bonds attributed to the two triangular faces coordinated with the transition metal Cd ions (Fig. 3C). Such 4c-2e σ bonds are reminiscent of cop-per-containing nonagermanide clusters such as $Cu(NHC)[Ge_9\{P(NH_2)_2\}_3]^-$ and $Cu[Ge_9\{P(NH_2)_2\}_3]$ and the first sandwich compound with the heteroatomic metal planar fragment, $\{(Ge_9)_2[\eta^6\text{-}Ge(PdPPh_3)_3]\}^{4-}$ [43,44]. Finally, the remaining 36 electrons can be localized on 18 5c-2e Sn5 σ bonds with ON = 1.77–1.97 (Fig. 3D). In general, the title clusters can be viewed as the Cd ions bridging two Sn$_9$/Ni@Sn$_9$ fragments [42].

In conclusion, we present two metal clusters, $[Sn_9CdSn_9]^{6-}$ (**1a**) and $[(Ni@Sn_9)Cd(Ni@Sn_9)]^{6-}$ (**2a**) which contain two Sn_9^{4-} and $Ni@Sn_9^{4-}$ subunits bridged by the Cd atom. The Ligand-free ternary Zintl anion $[(Ni@Sn_9)Cd(Ni@Sn_9)]^{6-}$ is the first heterometallic cluster that transition metal atom connects two $[M@E_9]^{q-}$ subunits. In our view, the Sn_9^{4-} and $Ni@Sn_9^{4-}$ gradually replaced the Mes-ligands of the CdMes$_2$ to form clusters **1a** and **2a** with sandwich structures. DFT calculations indicate that larger cluster fusion can be modulated by electronic structure.

Declaration of competing interest

The authors declare that they have no known competing financial interests or personal relationships that could have appeared to influence the work reported in this paper.

Acknowledgments

This work was supported by the National Natural Science Foundation of China (Nos. 92161102 and 21971118) and the Natural Science Foundation of Tianjin City (Nos. 20JCYBJC01560 and B2021202077) to Z.-M. Sun.

Supplementary materials

Supplementary material associated with this article can be found, in the online version, at doi:10.1016/j.cclet.2022.02.013.

References

[1] D. Sun, A.E. Riley, A.J. Cadby, et al., Nature 441 (2006) 1126–1130.
[2] M.M. Bentlohner, M. Waibel, P. Zeller, et al., Angew. Chem. Int. Ed. 54 (2015) 1–6.
[3] B. Peters, N. Lichtenberger, E. Dornsiepen, S. Dehnen, Chem. Sci. 11 (2020) 16–26.
[4] R.J. Wilson, N. Lichtenberger, B. Weinert, S. Dehnen, Chem. Rev. 119 (2019) 8506–8554.
[5] J. Zhao, Q. Du, S. Zhou, V. Kumar, Chem. Rev. 120 (2020) 9021–9163.
[6] J. Campbell, H.P.A. Mercier, H. Franke, et al., Inorg. Chem. 41 (2002) 86–107.
[7] J.M. Goicoechea, S.C. Sevov, J. Am. Chem. Soc. 128 (2006) 4155–4161.
[8] Z.M. Sun, Y. Zhao, Y.J. Li, L. Wang, J. Cluster Sci. 20 (2009) 601–609.
[9] D.O. Downing, P. Zavalij, B.W. Eichhorn, Eur. J. Inorg. Chem. 6 (2010) 890–894.
[10] S. Scharfe, T.F. Fässler, Eur. J. Inorg. Chem. 8 (2010) 1207–1213.
[11] B.B. Zhou, M.S. Denning, C. Jones, J.M. Goicoechea, Dalton Trans. 9 (2009) 1571–1578.
[12] H. He, W. Klein, L.A. Jantke, T.M. Fässler, Z. Anorg. Allg. Chem. 640 (2014) 2864–2870.
[13] V. Hlukhyy, S. Stegmaier, L. van Wllen, T.M. Fässler, Chem. Eur. J. 20 (2014) 12157–12164.
[14] B.J.K. Witzel, W. Klein, J.V. Dums, M. Boyko, T.F. Fässler, Angew. Chem. Int. Ed. 58 (2019) 12908–12913.
[15] D. Rios, M.M. Gillett-Kunnath, J.D. Taylor, A.G. Oliver, S.C. Sevov, Inorg. Chem. 50 (2011) 2373–2377.
[16] F.S. Kocak, D.O. Downing, P. Zavalij, et al., J. Am. Chem. Soc. 134 (2012) 9733–9740.
[17] B. Kesanli, J. Fettinger, D.R. Gardner, B. Eichhorn, J. Am. Chem. Soc. 124 (2002) 4779–4786.
[18] C. Liu, L. Li, L.X. Jin, J.E. McGrady, Z.M. Sun, Inorg. Chem. 57 (2018) 3025–3034.
[19] L. Xu, S.C. Sevov, J. Am. Chem. Soc. 121 (1991) 9245–9246.
[20] A. Ugrinov, S.C. Sevov, J. Am. Chem. Soc. 124 (2012) 10990–10991.
[21] A. Ugrinov, S.C. Sevov, Inorg. Chem. 42 (2003) 5789–5791.
[22] D.F. Hansen, B.B. Zhou, J.M. Goicoechea, J. Organomet. Chem. 721-722 (2012) 53–61.
[23] A. Nienhaus, R. Hauptmann, T.M. Fässler, Angew. Chem. Int. Ed. 41 (2002) 3213–3215.
[24] K. Mayer, L.A. Jantke, S. Schulz, T.M. Fässler, Angew. Chem. Int. Ed. 56 (2017) 2350–2355.
[25] L. Yong, M.B. Boeddinghaus, T.F. Fässler, Z. Anorg. Allg. Chem. 636 (2010) 1293–1296.
[26] F.S. Geitner, W. Kleinb, T.F. Fässler, Dalton Trans. 46 (2017) 5796–5800.
[27] J. Wang, B. Wahl, T.F. Fässler, Angew. Chem. Int. Ed. 49 (2010) 6592–6595.
[28] C. Zhang, H.W.T. Morgan, Z.C. Wang, Z.M. Sun, J.E. McGrady, Dalton Trans. 48 (2019) 15888–15895.
[29] M.M. Bentlohner, L.A. Jantke, T. Henneberger, et al., Chem. Eur. J. 22 (2016) 13946–13952.
[30] M. Kirchmann, K. Eichele, L. Wesemann, Inorg. Chem. 47 (2008) 5988–5991.
[31] M. Lutz, B. Findeis, M. Haukka, et al., Chem. Eur. J. 14 (2002) 3269–3276.
[32] B. Kesanli, J.E. Halsig, P. Zavalij, et al., J. Am. Chem. Soc. 129 (2007) 4567–4574.
[33] J.M. Goicoechea, S.C. Sevov, Angew. Chem. Int. Ed. 44 (2005) 4026–4028.
[34] A.D. Becke, Phys. Rev. A 38 (1988) 3098–3100.
[35] J.P. Perdew, Phys. Rev. B 33 (1986) 8822–8824.
[36] A. Schaefer, H. Horn, R. Ahlrichs, J. Chem. Phys. 97 (1992) 2571–2577.
[37] F.X. Pan, L.J. Li, Y.J. Wang, J. Am. Chem. Soc. 137 (2015) 10954–10957.
[38] M.S. Pasquette, L.F. Dahl, J. Am. Chem. Soc. 102 (1980) 6621–6623.
[39] L.R. Byers, L.F. Dahl, Inorg. Chem. 19 (1980) 680–692.
[40] L. Qiao, C. Zhang, C.C. Shu, et al., J. Am. Chem. Soc. 142 (2020) 13288–13293.
[41] D.Y. Zubarev, A.I. Boldyrev, Phys. Chem. Chem. Phys. 10 (2008) 5207–5217.
[42] T. Lu, F.W.M. Chen, J. Comp. Chem. 33 (2012) 580–592.
[43] N.V. Tkachenko, A.I. Boldyrev, Chem. Sci. 10 (2019) 5761–5765.
[44] H.L. Xu, N.V. Tkachenko, Z.C. Wang, et al., Nat. Commun. 11 (2020) 5286.